Simplifying drill-hole domains for 3D geochemical modelling: An example from the Kevitsa Ni-Cu-(PGE) deposit

Margaux Le Vaillant *, June Hill, Stephen J. Barnes

CSIRO Mineral Resources, Australia

ABSTRACT

A 3D geology model is a simplified version of the true geology, designed to give a visual summary of the geometry and distribution of major geological elements in a specified region. Drill holes provide detailed data of the subsurface that can be classified into geological units that are the fundamental elements of the 3D model. Due to software limitations, upscaling ('lumping') is usually required to reduce the number of geological units in the drill holes prior to model building. Upscaling is a subjective process, which means that different geologists will group in different ways and will typically not record the rationale behind their decision; this means the "experiment" is not reproducible. In our study we use a method of upscaling geological units, in this case based on assay data, using the continuous wavelet transform (CWT) and tessellation methods. This method reduces subjectivity and can easily be repeated (e.g. on an updated or new drill hole) by using the same parameters, ensuring that the upscaling process is consistent over all drill hole data. We apply this technique to a large assay database (>90,000 samples) from the Kevitsa Nickel-Copper-Platinum group element (PGE) deposit in Finland.

The Kevitsa Ni-Cu-(PGE) disseminated sulfide orebody is hosted in a Proterozoic layered intrusion in northern Finland. Internal geological subdivision and correlation within the intrusion is very difficult to do consistently using lithological observations, owing to general homogeneity of rock types and an overprint of alteration, but distinct variability is evident in Ni and PGE sulfide tenors. In its raw form, the tenor variation dataset appears noisy and unsystematic. We have applied the tessellation method to classifying ore types based on tenor variations, consistently and objectively reducing the number of units in each drill hole to create a simplified 3D model of the orebody. Our results reveal shallow inward dipping cryptic layering defined by sulfide composition, which are interpreted as reflecting an increase in Ni and PGE tenor with time during emplacement of the sulfide-bearing cumulates. We interpret this as a progressive increase in silicate-sulfide mixing efficiency (R factor) as the intrusion developed from an interconnected sill sediment-complex choked with country rock inclusions into a freely convecting magma chamber. Based on this case study, we show that the tessellation method can add considerable value by distinguishing the wood from the trees in large 3D geochemical databases. The method may be widely applicable in other Ni-Cu-PGE deposits where tenor variations appear, at first sight, to be chaotic and uninterpretable.

1. Introduction

Vast geochemical databases are commonly available from mining operations on ore deposits. These potentially contain a wealth of information with applications well beyond their immediate purpose of grade block definition and mine planning. In most deposit types such datasets can be interrogated to provide fundamental petrological and ore genesis information. Our research focuses on magmatic sulfide Ni-Cu-PGE deposits, and many examples show

the use of this approach, including studies of the Santa Rita Ni-Cu deposit in the Mirabela intrusion (Barnes et al., 2011) and the Voisey's Bay deposit in Labrador, Canada (Lightfoot et al., 2012). However, major challenges exist in distinguishing significant trends and patterns in very large datasets from the background of short range variability. The problem typically boils down to one: deciding at what scale to average and composite the data in order to optimally distinguish signal from noise. In this contribution, we describe a new method of analysis of large geochemical datasets specifically intended to address this problem. We illustrate the method by applying it to a very large mine assay database from

* Corresponding author.
E-mail address: margaux.levaillant@csiro.au (M. Le Vaillant).

the Kevitsa Ni-Cu-PGE deposit, to reveal petrologically significant cryptic variation within the deposit and its host intrusion.

The Kevitsa deposit in Arctic Finland is a large (237 Mt), low-grade disseminated Ni-Cu-(PGE) sulfide orebody (Santaguida et al., 2015) formed within a layered ultramafic-mafic intrusion that lacks obviously recognisable internal stratigraphy, with a rare visible layering and only an indistinct ratio layering (plagioclase/pyroxene) observed in one outcrop by Mutanen (1997). The host rocks to mineralisation are relatively homogeneous, pyroxene-dominated ultramafic cumulates containing irregular uncorrelatable units of variable olivine-enriched and xenolith-laden components containing small proportions of Ni-Cu-PGE bearing disseminated magmatic sulfides. Three different 'ore types' varying in Ni and PGE tenors have been described in the literature with very broad spatial zonings (Mutanen, 1997). The very extensive multi-element assay database available at Kevitsa (92,164 analyses covering all the mineralised part of the intrusion) has potential to reveal correlatable cryptic layering within the orebody itself, from which variations in the metal content of the sulfide component (tenor) can be derived. In a first attempt to visualise this dataset, a simple classification based on S, Ni and Pd tenors was applied to the assay dataset and plotted in 3D. Subtle trends could be distinguished, but the dataset remained very noisy and difficult to interpret. A novel domaining method was then applied to the data, producing a smoothed and de-noised result while remaining objective, thus revealing deposit-scale spatial patterns hidden within the data.

1.1. The spatial domaining approach

3D geology models allow geologists to understand the spatial distribution and geometry of geological units. For example in the North Karelia Schist Belt in eastern Finland, a study used 3D modelling combining multiple types of datasets to define the structure of the Outokumpu ore district and ophiolite hosted Cu-Co-Zn-Ni-Ag sulfide deposits (Saalmann and Laine, 2014). Drill hole data is a dominant source of information for building these models, and typically, the 3D geology models need to represent a simplified version of the geology in order to be of practical value. Indeed, the natural world is complex, and in order to answer specific questions, such as the distribution of Ni tenors within an ore body, simplification is necessary. Moreover, a less complex representation is often more representative of our level of knowledge, especially when considering data error and resulting uncertainties (Lindsay et al., 2012). One way to reduce the total number of geological units (i.e. upscaling) in the model is to perform "lumping" of the geological units in the drill hole data. Lumping involves aggregation of adjacent, similar geological units into spatial domains. In typical mine-site practise, units are manually aggregated by a geologist; however, this is a very time-consuming process and the results are subjective and non-repeatable. Therefore, we consider it highly desirable to be able to automate this process so that upscaling is rapid, consistent across the whole drill hole database and easily repeatable should new data become available.

In this contribution we describe a mathematical method for performing spatial domaining on numerical drill hole data, in this case the 90,000+ sample assay dataset from routine ore delineation drilling at Kevitsa. The user controls the degree of upscaling of the data via a filtering parameter which can be applied to the whole data set consistently. In our study, the geochemical dataset was the primary source of information to build the 3D model of ore variations within the intrusion, and three steps were considered in order to prepare the data prior to building the model: 1) choose a level of spatial domaining of the drill hole variables that is suitable for the model to be built; 2) combine the spatial domains for all the variables required for classification; 3) classify the com-bined spatial domains using the mean values of all the variables for each spatial domain. We show how this methodology applied at Kevitsa reveals cryptic chemical stratigraphy and lateral variability, with important implications for the grade and tenor distribution with the deposit, the emplacement history of the host intrusion and the origin of the orebody.

2. Kevitsa geology and mineralisation

The 2.058 Ga Kevitsa intrusion (Mutanen, 1997; Mutanen and Huhma, 2001) is located in the Central Lapland greenstone belt in northern Finland (Fig. 1a). It is part of a suite of small to medium sized mafic-ultramafic intrusions, including the large Koitelainen layered intrusion (Mutanen, 1997) as well as the neighbouring Sakatti intrusion hosting the Cu-Ni Sakatti deposit (Ahtola et al., 2012). These intrusions range in age from 2.1 Ga to 1.8 Ga (Huhma et al., 2013). They are emplaced into a volcanic suite comprising komatiites (Hanski et al., 2001; Heggie et al., 2013) basalts and rhyolites, intercalated with a thick sequence of locally sulfidic and graphitic, quartzitic to pelitic sedimentary rocks (Hanski et al., 2005).

The Kevitsa intrusion occupies a surface area of approximately 16 km^2 and consists of a lower ultramafic unit up to 2 km in thickness, overlain in an uncertain relationship by a mafic unit over several hundred metres thick (Fig. 1 – green unit). The ultramafic unit is composed of interlayered olivine pyroxenite and websterite, with local development of cyclic units, but for the most part lacking obvious internal layering (Santaguida et al., 2015). The mafic unit is made up of gabbro, ferrogabbro, and magnetite gabbro (Mutanen, 1997).

The Kevitsa Ni-Cu-(PGE) deposit, also referred to in the literature as the Kevitsansarvi deposit (Gervilla and Kojonen, 2002), occurs in the middle part of the ultramafic unit, associated with variably layered olivine pyroxenites and websterites. The Kevitsa deposit consists entirely of disseminated sulfides with widely varying Ni, Cu and PGE tenors (Fig. 2), with a published combined resource of 237 Mt at 0.28% Ni, 0.41% Cu and 0.6 ppm 3E (Pt + Pd + Au) (Geological Survey of Finland website, 2016) with Ni grades up to around 0.6% (99th percentile on all assays in the database). Mine geologists have separated the mineralisation into different ore types, mainly on the basis of their Ni-PGE tenors. Low tenor ores which form near the base of the intrusion and along the margins of the Cu-Ni mineralization, but are also found internally are classified as "false ore". This pyrrhotite-rich mineralisation, dominantly disseminated but locally net-textured and semi-massive at the decimetre scale, is often associated with country rock xenoliths. The "normal ore" (or Cu–Ni ore type) represents the bulk (>90%) of the economic resource and is characterised by 2–6 vol% of sulfides (pyrrhotite, pentlandite, and chalcopyrite) and average Ni and Cu ore-grades of 0.3 and 0.4 wt% respectively (Santaguida et al., 2015). Finally, the "Ni–PGE ore", which occurs more locally, has a similar sulfide content to that of the Normal ore, but the sulfides are predominantly pentlandite, pyrite and millerite, and the ores have higher and more variable Ni grades, lower Cu grades (Ni/Cu = 1.5–15), and extreme Ni tenors in excess of 30%. Extremely high Ni contents are developed within olivine grains in the Ni-PGE ores (Yang et al., 2013). It is likely that these Ni-PGE ores constitute another example of extremely high Ni tenor ores related to formation from Ni-enriched magmas at high values of silicate to sulfide mass ratio (R factor) in the presence of olivine (Barnes et al., 2013).

The greenstone sequence and the Kevitsa intrusion were metamorphosed and hydrothermally altered during regional greenschist facies metamorphism (Mutanen, 1997), producing various alteration zones and cross-cutting veins within the orebody.
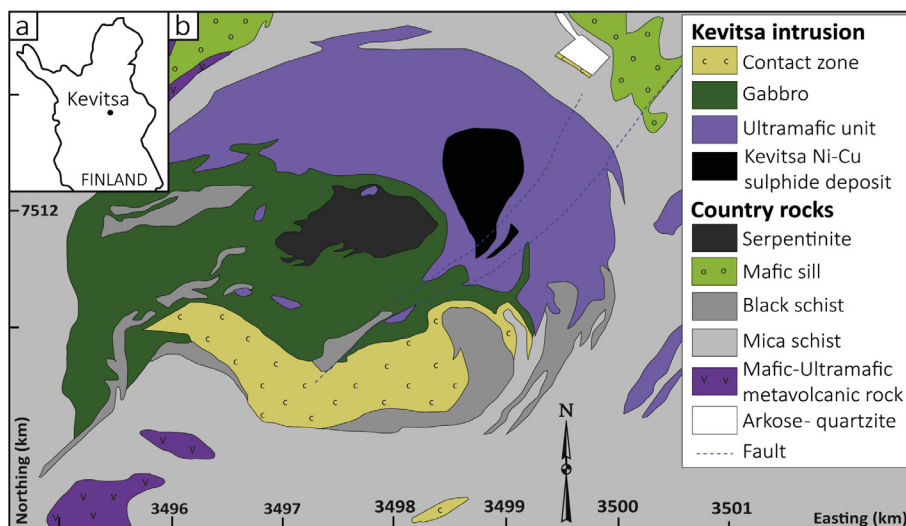
Fig. 1. A) Location of the Kevitsa intrusion in the Central Lapland greenstone belt, northern Finland (after Hanski et al., 2001). B) Simplified geological map of the Kevitsa intrusion (after Mutanen, 1997). Figure taken from Le Vaillant et al., 2016.
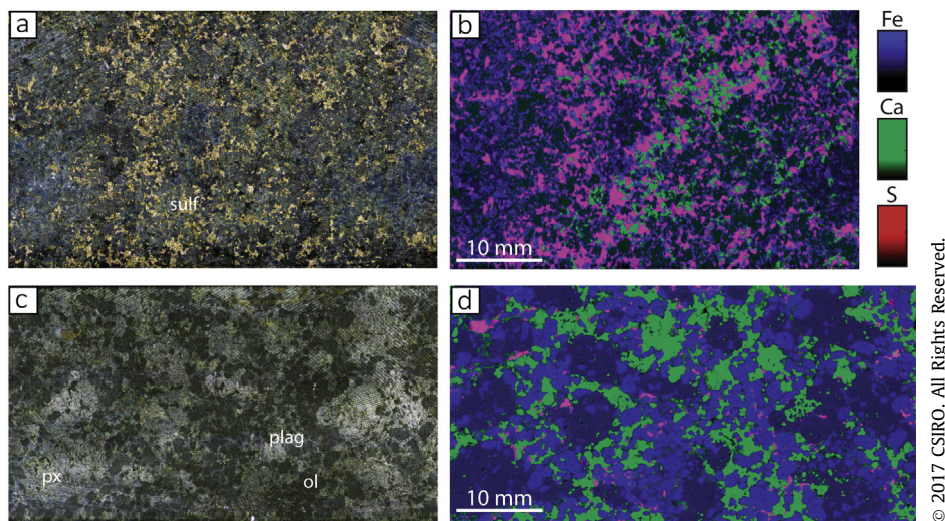
Fig. 2. Illustrations of the mineralisation at Kevitsa. a) and b) are photomicrographs of mineralised pyroxenites, and c) and d) are 3 elemental maps (Fe, Ca and S) of these respective samples. These micro-XRF maps were collected on the Bruker Tornano micro XRF mapper at ARRC, Kensington, Western Australia; these chemical maps are false colour images, each element normalized to maximum abundance. (For interpretation of the references to colour in this figure legend, the reader is referred to the web version of this article.)

Detailed study of these veins (mainly quartz, carbonate or chlorite/epidote veins) reveals that they play only a minor role in redistributing primary metal concentrations (Le Vaillant et al., 2016).

3. Assay database

The Kevitsa assay database is supplied as geochemical analyses of representative samples of drill hole intervals. The size of the intervals may vary between drill holes but are usually approximately 1 m or 2 m in length. The database contains 92,164 analyses, providing concentrations in Ni, Cu, Co, S, and Au, obtained primarily by ICP-MS directly after aqua regia digest for Ni and Cu and by ICP-MS after Pb fire assay for Au, Pt and Pd. In addition, "NiS", "CoS" and "CuS" concentrations, the concentrations in the rock of the components of Ni, Cu and Co that occur within sulfide minerals, were also determined, to discriminate recoverable sulfide-hosted metals from the non-recoverable component contained with silicate minerals (mainly olivine). This determination was made after using a citric acid digest on the samples, which is weaker than the aqua regia digest, and only dissolves metal sulfides (as well as carbonates, which are mainly present within secondary veins at Kevitsa and do not contain metals within the carbonate mineral phases). The whole rock content of sulfide-hosted Ni is referred to as "NiS" in the following data presentation. All the data used for this study can be found in report NI43-101 published on SEDAR (document required by the Canadian Securities Commission) in 2011.

4. Classification method

In a first attempt to visualise the Kevitsa assay dataset, a simple classification was defined in order to reproduce the different ore types used by the mine geologists, based initially on whole rock S, and NiS, refined using Pd and Ni tenors (concentration of Ni and Pd in 100% sulfide). The groupings for this initial classification are:

1) Non ore (S < 0.5 wt%)
2) "False ore" (high whole-rock S, low Ni concentrations),
3) Normal ore, representing the main bulk of the ore assays, subdivided in two types, (a) moderate Ni – low to moderate Pd and (b) moderate Ni – high Pd;
4) High Ni-PGE ore (elevated Ni and Pd concentrations in comparison to the main bulk of the ore).

This initial manual classification was applied to each analysis within the database, and it allowed us to distinguish cryptic variations in the 3D model. However, the model needed to be simplified to enable visualisation of large scale tenor variations within the system; hence upscaling was necessary. The tessellation technique (Hill et al., 2015) was used to "lump" units together into larger scale 1D spatial domains, which were then re-classified. The use of this technique provided us with an unbiased, simplified representation of the tenor variations within the mineralised part of the magmatic system, allowing us to visualise its geometry, and obtain insights on the genetic processes at play.

Within the base metals concentrated in sulfides present in the system (Ni, Co and Cu), Ni variations are more representative of primary magmatic variations; how much Ni is present within the sulfides is a function of mixing efficiency of the magma. The distribution of Cu would be more subject to late stage remobilisation, due to the demonstrably more mobile nature of Cu in this deposit (Le Vaillant et al., 2016). Nickel was therefore chosen as a representative element. At Kevitsa, there is an extremely good correlation between the concentrations of the various PGEs, as they appear to be unaffected by later hydrothermal remobilisation (Le Vaillant et al., 2016). Pd is therefore a good proxy to use to study the variations of PGE concentrations within the system, and it was chosen as a representative element. Finally, as stated previously in the description of the ore classification, we used the concentration of S to distinguish samples containing potentially ore grade sulfide minerals (potential ore) from non-ore material.

Once the tessellation technique has been used to 'lump' units together, the applied classification of ore types is based on Ni tenors, Pd tenors and S concentration. Nickel and Pd tenors represent the sulfide Ni (NiS) and Pd contents recalculated back to 100% sulfides. They were obtained using the following calculation:

$$Ni_{tenor} = 38 \times \frac{NiS_{pct}}{S_{pct}}$$

$$Pd_{tenor} = 38 \times \frac{Pd_{ppb}}{S_{pct}}$$

In these equations, 38 represents the assumed S content of the sulfides, representative of a typical magmatic sulfide assemblage composed of pyrrhotite, pentlandite and chalcopyrite. Normalisation to 38% S is preferred over more elaborate sulfide norm calculations (Barnes and Lightfoot, 2005) on the grounds that the accumulated uncertainty in the normalisation due to analytical error, minor mobility of S, possible presence of pyrite, silicate Ni background etc. overwhelm the ostensibly improved precision of the mode calculation (Kerr, 2001). Barnes et al. (2011) performed an error analysis on calculated tenors for the Santa Rita – Mirabela deposit in Brazil, and found that for samples with more than 1 wt% S, errors in calculated Ni tenors were around 15 wt% of the amount present, reducing to a constant 10 wt% for S contents greater than 1.5 wt%, but increasing sharply for S contents below 0.5 wt%. Much of the uncertainty in the Mirabela dataset stemmed from the fact that whole rock, rather than sulfide-bound Ni was used as the input, and hence the major error arose from uncertainty in the background silicate Ni content. In the Kevitsa case, having a direct analysis of sulfide bound Ni from the selective acid leach largely eliminates this source of error, such that reliable tenor estimates can be made at lower sulfide contents. In the data set considered here, the variability in Ni tenors for samples in the range 0.5–1 wt% S is not detectably greater than that in the range >1 wt% (Appendix Fig. 1), which we take as justification for using 0.5 wt% S as the lower limit for reliable tenor calculation. Extrapolation to 100% will of course involve a twofold decrease in the precision of the tenor estimate for 0.5 as opposed to 1 wt% S, but this imprecision appears to be insignificant compared to the natural variability in the data.

Figure 3 shows the division chosen for the different ore classes based on the re-classification of the database after the tessellation had been applied on the data:

1) Low sulfur, S < 0.5 wt% (no ore),
2) high S (S < 0.5 wt%) Low Ni tenor (equivalent of the false ore – Ni tenor <2 wt%), and then 3 more classes forming a continuum from
3) low Pd tenor (Pd tenor < 1500 ppm)-moderate Ni tenor (2 wt% < Ni tenor < 10 wt%),
4) high Pd tenor (Pd tenor > 1500 ppm)-moderate Ni tenor (2 wt% < Ni tenor < 10 wt%), and
5) high Pd and high Ni tenors (equivalent of the high Ni-PGE ore type – Ni tenor > 10 wt%).

5. Spatial domaining and upscaling

Classification of drill hole samples from geochemistry (or any downhole measurement) without reference to spatial information typically results in a very noisy classification when plotted against drill hole depth (for example, Hall and Hall, 2017). The aim of this experiment is to produce a 1D spatial domaining of the drill hole data which simplifies the process of building a 3D geological model for the Kevitsa deposit. A method of upscaling the lithogeochemical units is required which preserves the location of major lithogeochemical boundaries. It is required that the upscaling be an iterative process so that upscaling can be performed at progressively higher levels until a result is produced which is suitable for generating a 3D model. Multiscale spatial domaining techniques, described below, can be used to provide a basis from which to select a suitable up-scaled model of the data. A flowchart of the domaining and multivariate classification process used here is shown on figure 4. A summary of the algorithm is provided in Appendix 2 and more detail can be found in Hill et al. (2015).

The continuous wavelet transform (CWT) is a mathematically efficient method of producing multiscale spatial domaining (Mallat, 1991; Mallat and Hwang, 1992; Mallat and Zhong, 1992) and has been used for detecting boundaries in stratigraphic sequences from wireline logs (Arabjamaloei et al., 2011; Cooper and Cowan, 2009; Davis and Christensen, 2013; Panda et al., 2000; Perez-Muñoz et al., 2013). The results of CWT are usually illustrated using a scale-space plot (also called a scaleogram), however, this representation is difficult to interpret. Alternatively the results can be represented in a simplified format called a tessellation (Hill et al., 2015; Witkin, 1984) and in this form it can be filtered to remove weak features (i.e. features which represent small amplitude changes in the signal (Hill et al., 2015)). In this paper, we demonstrate the use of progressive filtering of the tessellation to perform upscaling of the lithological domains. This is a very useful method since 1) computation is fast, 2) it provides an intuitive multiscale visualisation, and 3) it allows different levels of filtering (upscaling) for different variables. Domains created by the tessellation for different variables can be merged to provide multivariate domaining. The upscaling process is independent of the classification method chosen. For the purposes of this paper we use an expert-derived manual classification (as described in
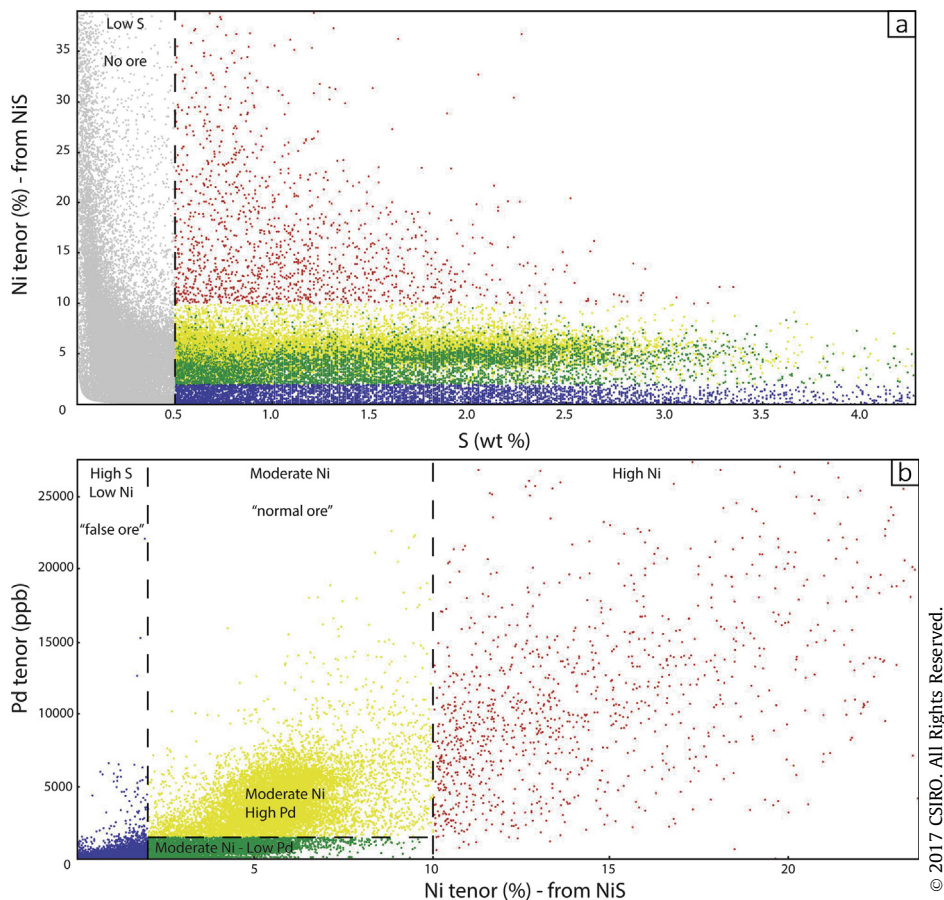
Fig. 3. Classification of samples using 3 variables: S wt%, Ni tenor (calculated from NiS) and Pd tenor. a) Shows the separation between "no ore" (S < 0.5 wt%), and the mineralised samples, b) shows the divisions between the different ore types.
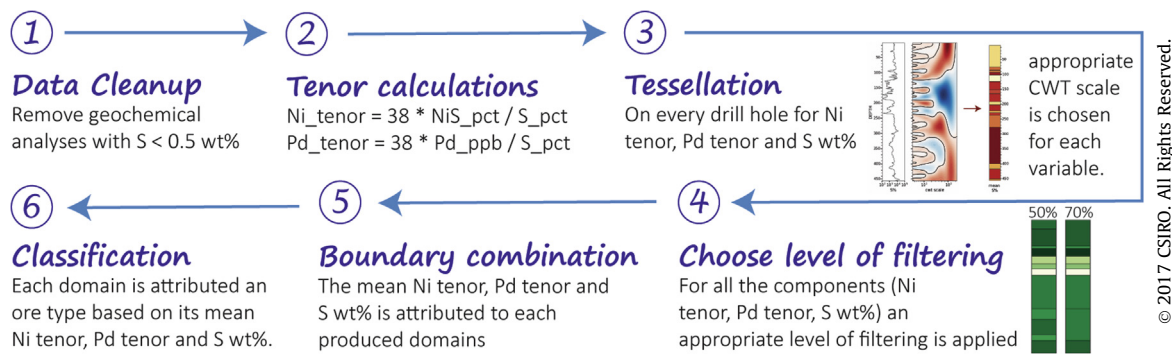

Fig. 4. Flow chart of the domaining and multivariate classification workflow.

the previous section), but any classification method could be used on the merged domains. The CWT-tessellation method is described in more detail in the next section.

The steps are as follows:

1. A small subset of drill holes is chosen for determining appropriate filter levels.
2. The tessellation for each variable in the test set is computed and then filtered until the smallest scale representation is suitably upscaled. An example for one variable is shown in figure 5.
3. The results of different filter levels are compared (Fig. 6). When visual inspection indicates that the results have performed an acceptable upscaling, the filter for each variable is applied to

the full drill hole data set, resulting in a consistent level of upscaling across the entire data set.
4. The boundaries for all the variables (in our case, Ni tenor, Pd tenor and S wt%) are merged (Fig. 7).
5. The mean values for each of the merged variables in each combined domain is used in the multivariate classification; i.e. the tenor-based classification scheme shown in figure 3 is applied to these mean values, to obtain a classification for the whole domain. Adjacent domains which have the same classification label are merged into a single domain (Fig. 7).

Equivalent filters were applied to each variable in this experiment, however, different filter levels can be applied to each
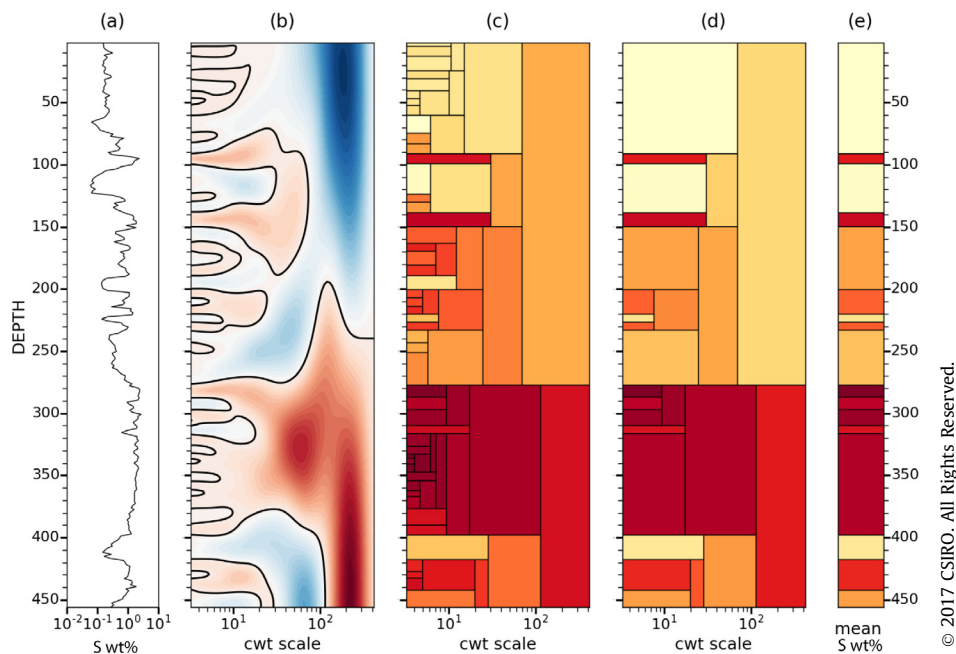
Fig. 5. (a) S wt% plotted down hole for KV155, x-axis is log scale, depth in metres. (b) Scale-space plot for the continuous wavelet transform for the second derivative of Gaussian wavelet. Colours represent the wavelet coefficients, with stronger colours representing higher absolute values (blue and red correspond to low and high S regions, respectively); the black line is the zero contour. (c) Tessellation of the second order scale-space plot in (b). Colours represent mean values of samples over the depth range represented by each domain; colour map of pale yellow to red corresponds to increasing mean S wt%. (d) Filtered tessellation (50% filter), resulting in removal of weak features. (e) Single scale log extracted from the filtered tessellation (i.e. at the smallest scale of the tessellation); this represents an upscaling of the S wt% domains. (For interpretation of the references to colour in this figure legend, the reader is referred to the web version of this article.)
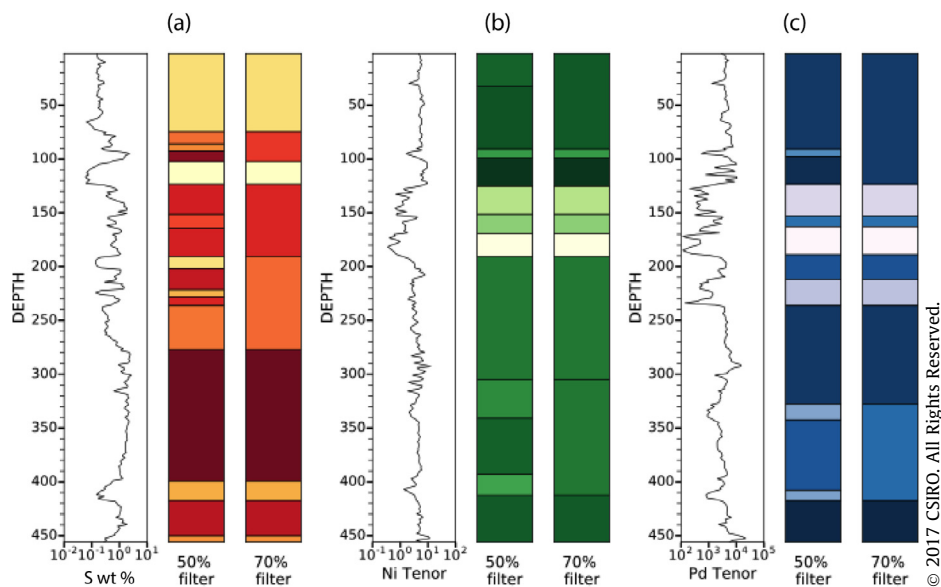

Fig. 6. Effect of up-scaling the tessellation by 50% and 70% filtering of KV155: (from left to right) S wt%, Ni tenor and Pd tenor. Pale colours represent low values of the geochemical element or ratio, and deep colours represent high values. (For interpretation of the references to colour in this figure legend, the reader is referred to the web version of this article.)

variable if required (i.e. to Ni tenor, Pd tenor and S wt%). The effects of applying various levels of filtering on the final classification for one drill hole are shown in figure 8. For our study, once a suitable level of filtering was selected, the entire drill hole assay data base was processed with the exception of drill holes which had less than 20 m of assay samples or were less than 50 m in total length as these will contribute little useful information to the final large scale 3D model. The total length of drill hole samples processed by this method was approximately 140 km, representing about 70% of the entire mine site drill hole database.

5.1. The continuous wavelet transform and tessellation

The CWT provides a computationally efficient method for calculating the locations of edges (singularities) in a signal at a range of scales (Mallat, 1991). In this example, the signal is the sequence of depth attributed assay values. Scale refers to the size of the neighbourhood where the signal changes are computed (i.e. the width of the wavelet). The concept of multi-scale comes from the range of scales that are used in the CWT, with the smallest scale typically being the length of 2 sample intervals. This means that for a 1 m
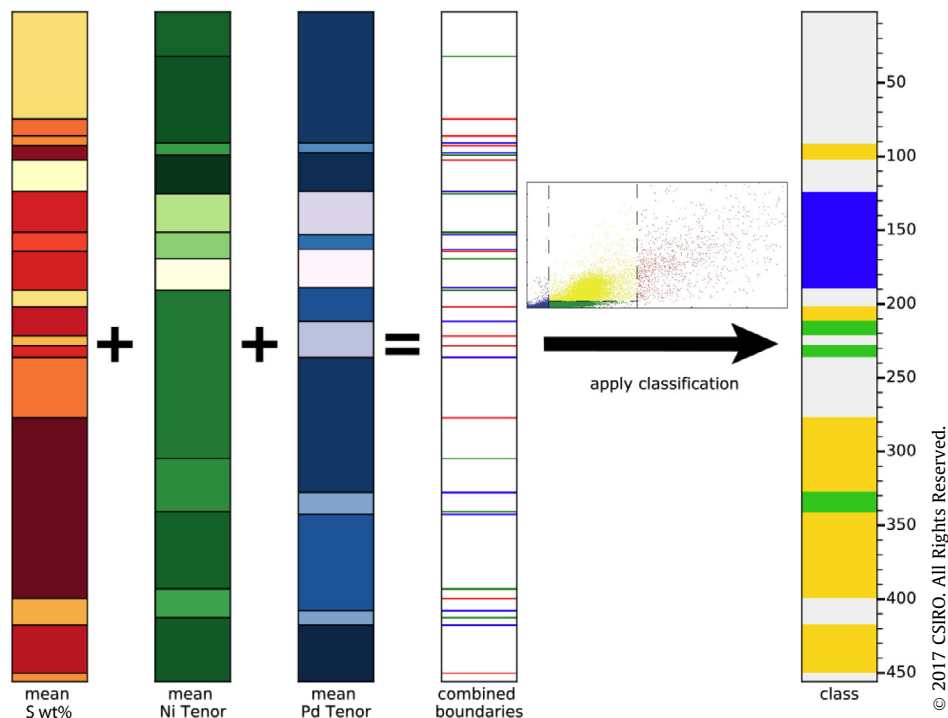
Fig. 7. Combined boundaries for up-scaled domains for 3 variables (S wt%, NiS tenor and Pd tenor). Domains between combined boundaries are then classification using proposed scheme.
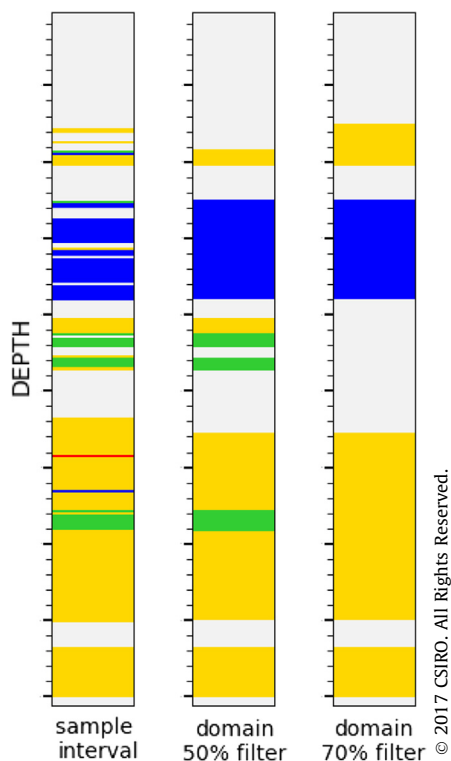

Fig. 8. Effect of up-scaling by tessellation filtering on drill hole classification of KV155: (from left to right) original sample; 50% filter up-scaling; 70% filter upscaling. Colour scheme is same as figure 7. (For interpretation of the references to colour in this figure legend, the reader is referred to the web version of this article.)

sampling interval, the minimum domain size is 2 m wide. The boundaries are detected using a second-order derivative of

Gaussian (DOG) wavelet to locate the inflection points in the signal (Mallat and Hwang, 1992). The DOG wavelet also acts as a smoothing function, the width of the wavelet increases with increasing scale. The method described by Torrence and Compo (1998) is used to calculate the CWT. The results of the CWT are typically displayed as a scale-space plot, figure 5 shows an example scale-space plot. In this example, "space" is depth down hole. The zero contours of the second order DOG wavelet are highlighted in black; these are the inflection points in the signal and represent the location of geochemical change at that scale.

The scale-space plot can be difficult to interpret as the location of values at large scales can be disturbed by interference from neighbouring features in the signal. The tessellation provides a compact and intuitive visualisation of the scale-space plot (Hill et al., 2015) because it uses the localisation assumption of Witkin (1984): that the true location of the inflection point is given by the location of the zero contour as the scale approaches zero. Hence the boundaries on the tessellation are plotted at the depth where the zero contours intersect the smallest scale in the scale-space plot. In the tessellation plot domains are represented by rectangles. Each rectangle is coloured by the mean value of the samples over the depth represented by the rectangle.

Filtering of the tessellation is based on wavelet coefficients. Filtering removes domains whose absolute maximum wavelet coefficient is below a selected threshold (Hill et al., 2015), this results in the removal of weak features. The level of threshold is selected by the user, empirically, and is based on the level of filtering required for the application. Filtering retains the hierarchical, multiscale nature of the tessellation but reduces the number of rectangles. Filtering can be used as a method of upscaling; it tends to retain small features that have a strong signal, which may be lost when scale thresholding is used as an upscaling method. When dealing with mineral deposits, it is important to preserve small scale but strongly enriched features. Final results of the domaining and upscaling using the tessellation technique are presented in 3D in figure 9.
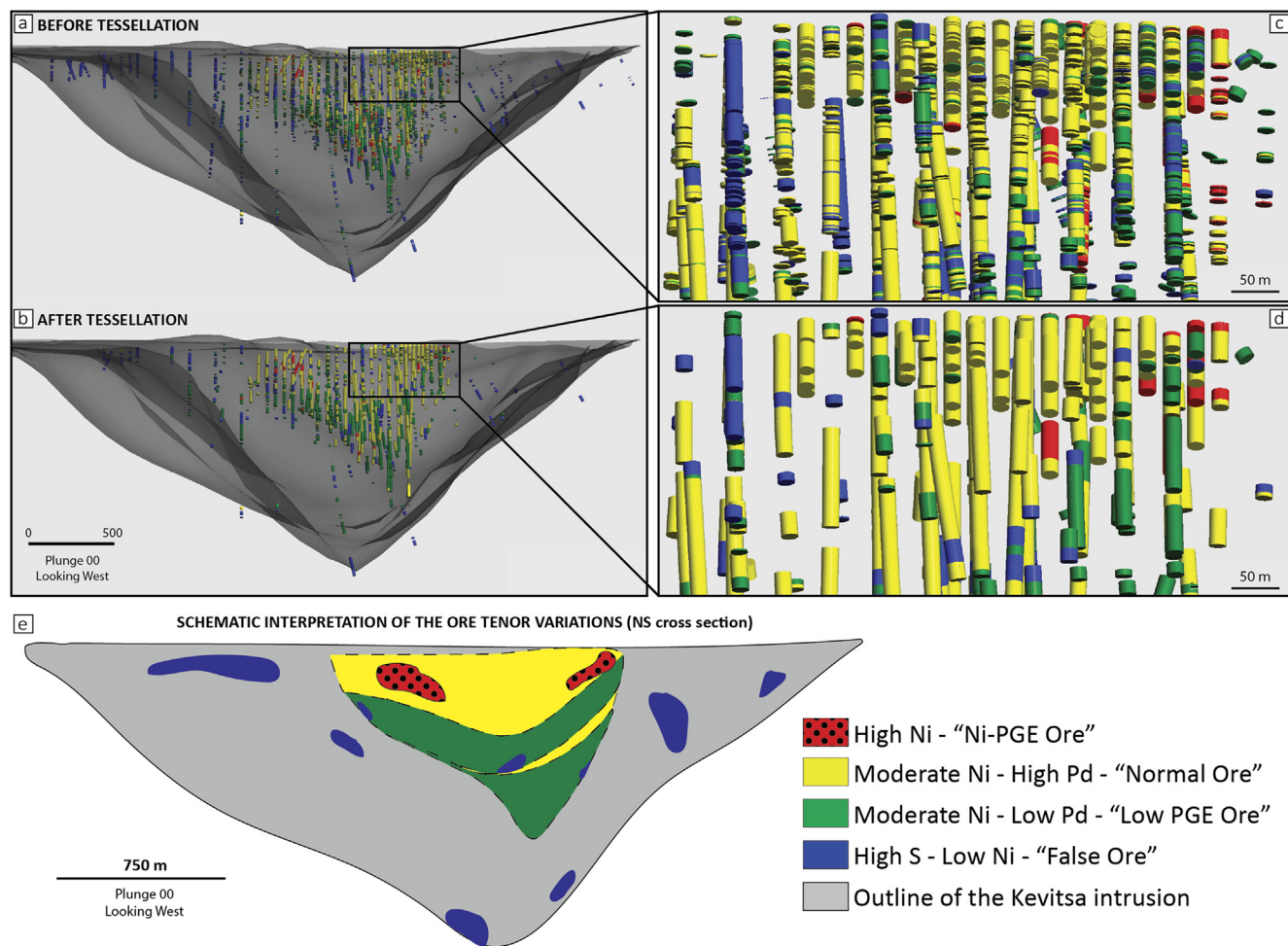
Fig. 9. View from the East of a slice through the Kevitsa 3D model before (a) and after (b) the tessellation process. c) and d) show zoomed in areas of both of these models. e) Schematic interpretation of the ore tenor variations on a NS cross section (same orientation as the 3D model shown above.

6. Discussion

6.1. The domaining and upscaling method

Domaining and upscaling using the tessellation technique allowed us to consistently and objectively reduce the number of units in each drill hole, and create a simplified 3D model of the orebody (Fig. 9). An obvious zonation can then be observed, with an increase of the sulfide tenors (both Ni and Pd) from the bottom towards the top of the ore body, with trends going from moderate Ni – low Pd, to moderate Ni – high Pd, up to zones of high Ni – high Pd ore towards the top of the ore body. The boundaries between the moderate Ni – low Pd zone and the moderate Ni – high Pd zone define roughly conformable inward-dipping layers. The high S, low Ni samples ('False ore') seem to be more concentrated on the edges of the mineralisation and closer to the sides of the intrusion. The genetic implications of these spatial variations in tenors will be discussed below.

6.2. Geological interpretation of upscaled data

After domaining and upscaling of the Kevitsa assay database, using a very strong filter (70%), the spatial distribution of the various ore types defines a shallow inward dipping cryptic layering. This layering is defined by variations in Ni and Pd tenors of the sulfides, with a general increase in Ni and PGE tenors from the bottom towards the top of the intrusion (Fig. 9).

Metal enrichment of sulfides is recognized to be the result of interaction between sulfide droplets and silicate melt. The more interaction there is, the more chalcophile elements have time to be transferred from the silicate melt into the sulfides, therefore increasing their metal tenors. This increase of interaction can be due to either (1) an elongation of the transport pathway of the sulfides, or (2) an augmentation of the volume of silicate melt with which the sulfides equilibrate through more efficient stirring and break-down of compositional boundary layers within freely convecting magma (Mungall, 2002). Another possible interpretation of the increase of metal tenors of the sulfides from the bottom towards the top of the intrusion would be (3) that the Kevitsa intrusion is composed of the accumulation of a series of sill-like intrusions containing sulfides with increasing metal tenors. In this case, the change in tenors of the sulfides would be happening further down at depth in the magmatic system, before the sills intrude the crust. This hypothesis invokes similar processes to the ones at play with a simple expansion of the intrusion itself, but requires more assumptions involving fortuitous timing of the emplacement history.

We favour the second hypothesis (Figs. 10 and 11), increasing mixing efficiency in an expanded magma chamber leading to higher effective R factors, on the grounds of simplicity. An increase of the length of the transport pathway of the sulfide with time (model 1) would suggest a change in the sulfur source with time, which represents a more complicate explanation, and as explained above, the hypothesis of accumulation of sill like intrusions
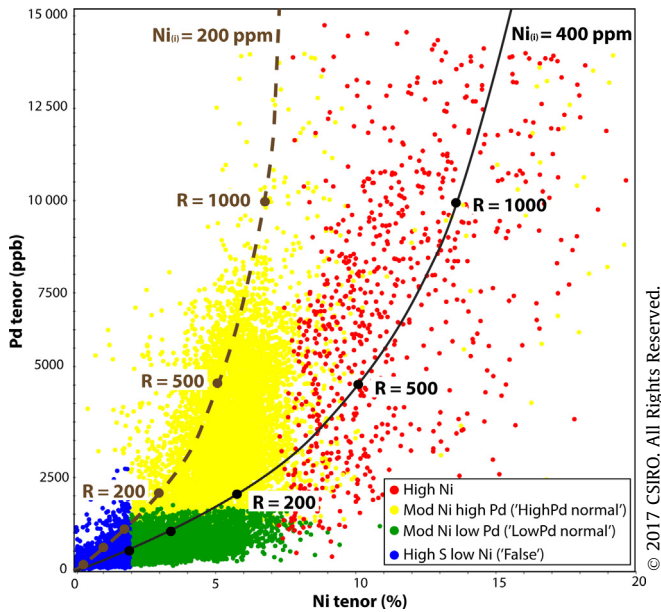
Fig. 10. Evolution of the ore tenors within the Kevitsa mineralisation in function of R factor.

(model 3) requires assumptions involving more complicated fortuitous timing of processes at play.

Our interpretation of the observed increase in metal tenors within the Kevitsa intrusion is explained by the following sequence of events. The magmatic system started as an interconnected sill sediment-complex choked with country rock inclusions (Fig. 11 – step 1). At this stage, the wholesale assimilation of country rocks, combined with a limited amount of stirring, triggered the production of high S - low tenor sulfides, or 'False ore'. With time, the system developed in a larger magmatic chamber, due to a continuous flux of magma being pumped into the system, allowing for more convection of the magma (Fig. 11 – step 2 and 3). At this stage, the sulfide droplets which would have been produced by the assimilation of S rich country rocks by the magma, interacted with larger volumes of magma, enriching them in Ni and PGEs. As the magmatic system evolved towards a freely convecting magma chamber, the sulfides became more and more enriched in Ni and PGEs through higher effective R factors and became trapped in the cumulates that accumulated from the bottom up. A distinctive type of poikilitic net-texture in the Kevitsa ores resulted from limited percolation of interconnected sulfide liquid networks though the intercumulus pore space (Barnes et al., 2017) but the scale of this process was not large enough to disrupt the cryptic layering. The gentle inward dipping that we observe now could be partially primary, reflecting the distribution of isotherms within the intrusion, or could be the result of syn-emplacement deformation of the country rocks accommodating the isostatic loading of a dense body of ultramafic rocks. Both processes were probably coupled with some post emplacement tectonism.

A few scattered domains of extremely high Ni and PGE tenors are present towards the top of the mineralisation. These have been interpreted by Yang et al. (2013) as the product of assimilation of massive or semi-massive sulfides associated with komatiitic rocks present in the country rocks, locally elevating the Ni content of the magma. Assimilation of blocks of locally distinct contaminant would account for the intermittent distribution of the high
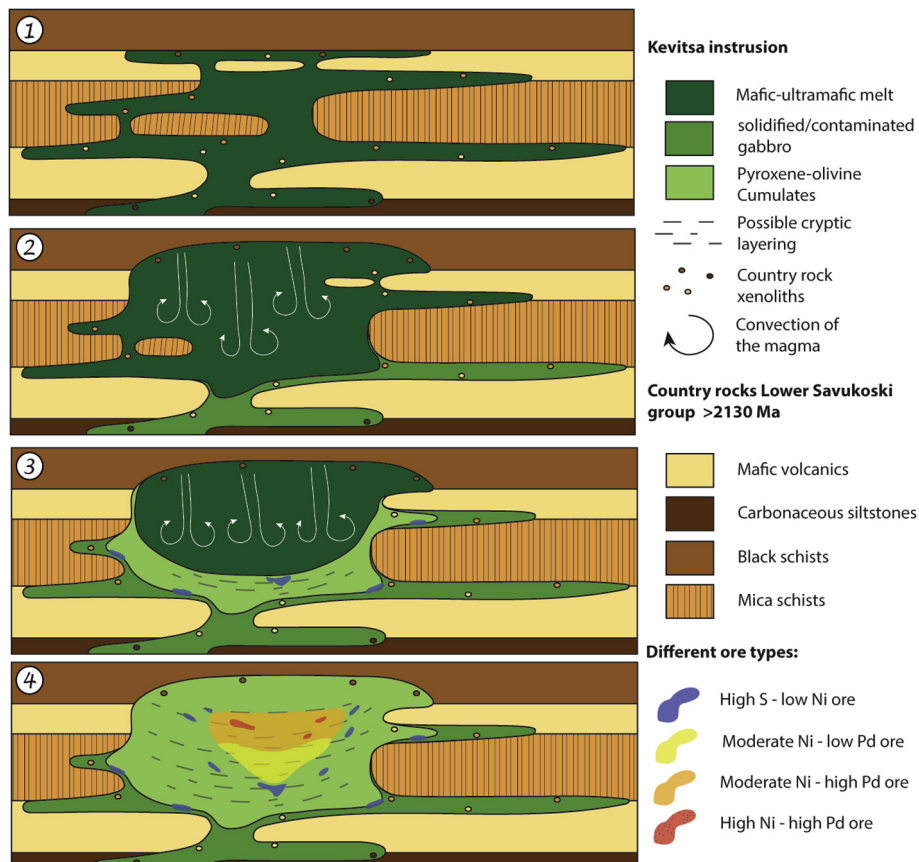

Fig. 11. Representation of the genetic model discussed here for the Kevitsa mineralised intrusion.

Ni-PGE ore domains. Where more xenoliths are present, patches of low tenor sulfides form ('false ore') and these patches can be observed in the 3D model all around the main mineralised body, as well as on the edges of the intrusion (Fig. 9). These are relics of an early phase of emplacement of a viscous, slow-flowing sludge of magma and disaggregating sulfidic xenoliths; this sludge stopped flowing before the xenoliths had time to melt and fully release their sulfide component.

6.3. Other applications of the upscaling method

For our purposes we have applied a very strong filter to extract only the coarsest of features from this data set. However, the multiscale information provided by the method has the potential to provide a more sophisticated result. For example, a simplified 3D orebody model can be generated using the coarse upscaling (in the current study, Leapfrog®|Geo was used as the main 3D visualisation and modelling software). This can be done rapidly by using implicit modelling software. From this model, any 3D region of particular interest, e.g. a high grade orebody, can be extracted and populated with finer scale results to produce a local detailed model of the ore distribution; i.e. with a lower percentage filter applied.

This method has the advantage over conventional compositing of drill hole data in that compositing occurs over a fixed length. Domaining using CWT and tessellation results in domains whose size is a reflection of the location of major changes in the variable values. So large regions in which there is very little change in the value of a variable will be lumped into a single domain, while narrow regions that contain values in strong contrast to their neighbourhoods will be preserved. This is particularly useful for identifying narrow regions of high grade or unusual composition.

Combining variables by combining their boundaries also has other potential benefits as boundaries have no measurement unit and no resolution. Therefore boundaries derived from different types of drill hole measurements taken at different resolutions could potentially be combined, for example, boundaries from a wireline logging variable could potentially be combined with those from a chemical element. This would make an interesting subject for future study.

7. Conclusion

In this study, the tessellation method added considerable value to the interpretation of the processes at play during the genesis of the Kevitsa ore body. This domaining and upscaling technique allowed us to distinguish the essential parts of the signal from the unwanted "noise" in this large 3D geochemical database. The method may be widely applicable in other Ni-Cu-PGE deposits where tenor variations appear at first sight to be chaotic and uninterpretable. Spatial domaining and filtering using the tessellation of the continuous wavelet transform provides a very rapid and efficient method for upscaling, which can be applied to large data sets in a consistent way by removal of weak (low amplitude) features that represent unwanted noise. This is a significant improvement over manual methods, which will be slow and inconsistent, or by universal removal and replacement of all small features, regardless of their significance.

Appendix 1: Figure showing the reasoning behind the use of a 0.5 wt% S threshold

Ni tenor versus Pd tenor logged plots showing that the variability in Ni tenors for (1) samples in the range 0.5–1% (data set plotted on diagrams c and d which include samples between 0.5 and 1 wt% S) is not detectably greater than that in the range S > 1 wt% (2) (data set plotted on diagrams a and b which include only samples with S > 1 wt%).

Appendix 2: Programming

The domaining algorithm was programmed using Python programming language. The following steps were used:

1. Data preparation:
   - Removed samples with invalid or missing data or with less than 20 samples.
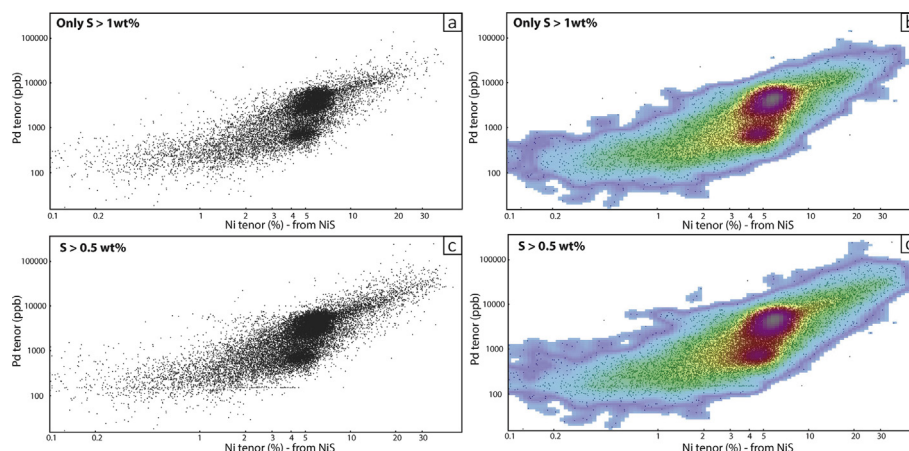   - Regularise sample intervals (required for the wavelet transform).

Fig. A1.

2. Run continuous wavelet transform on selected variables from drill holes using 2nd order derivative of Gaussian wavelet following the method of Hill et al. (2015).

3. Run tessellation on wavelet coefficients for each variable and each drill hole following the method of Hill et al. (2015).

4. Filter tessellation until desired upscaling of domains is achieved for the minimum scale of the wavelet transform (use consistent filter parameters for all drill holes) following the method of Hill et al. (2015).

5. Combine domains for all variables:
   - Make new domains from combining domain boundaries from all variables.
   - Fuse boundaries which are very close (2 samples or less).

6. Classify the domains using the mean values for each variable and a suitable classification system.

7. Combine adjacent domains which have the same class.

References

Ahtola, T., Eilu, P., Kärkkäinen, N., Tiainen, M., Tontti, M., Äikäs, O., Halkoaho, T., Kontinen, A., Kuivasaari, T., Nikander, J., Pohjolainen, E., Sorjonen-Ward, P., Torppa, A., Västi, K., Kontoniemi, O., Heikura, P., Hulkki, H., Iljina, M., Juopperi, H., Karinen, T., Konnunaho, J., Korkiakoski, E. A., Kyläoski, M., Niiranen, T., Nykänen, V., Räsänen, J., Makkonen, H., Korsakova, M., and Perdahl, J.-A., 2012. Metallogenic areas in Finland: Special paper – Geological Survey of Finland, vol. 2012, pp. 207–342.

Arabjamaloei, R., Edalatkha, S., Jamshidi, E., Nabaei, M., Beidokhti, M., Azad, M., 2011. Exact lithologic boundary detection based on wavelet transform analysis and real-time investigation of facies discontinuities using drilling data. Pet. Sci. Technol. 29, 569–578.

Barnes, S.-J., Lightfoot, P.C., 2005. Formation of magmatic nickel sulfide deposits and processes affecting their copper and platinum group element contents. Econ. Geol. 100th Anniversary Volume, 179–214.

Barnes, S.J., Godel, B., Gurer, D., Brenan, J.M., Robertson, J., Paterson, D., 2013. Sulfide-olivine Fe-Ni exchange and the origin of anomalously Ni-rich magmatic sulfides. Econ. Geol. 108, 1971–1982.

Barnes, S.J., Mungall, J.E., Le Vaillant, M., Godel, B., Lesher, C.M., Holwell, D.A., Lightfoot, P.C., Krivolutskaya, N.A., Wei, B., 2017. Sulfide-silicate textures in magmatic Ni-Cu-PGE sulfide ore deposits. 1. Disseminated and net-textured ores. Am. Mineral. 102, 473–506. http://dx.doi.org/10.2138/am-2017-5754.

Barnes, S.J., Osborne, G.A., Cook, D., Barnes, L., Maier, W.D., Godel, B., 2011. The Santa Rita nickel sulfide deposit in the Fazenda Mirabela intrusion, Bahia, Brazil: Geology, sulfide geochemistry, and genesis. Econ. Geol. 106, 1083–1110.

Cooper, G.R., Cowan, D.R., 2009. Blocking geophysical borehole log data using the continuous wavelet transform. Explor. Geophys. 40, 233–236.

Davis, A.C., Christensen, N.B., 2013. Derivative analysis for layer selection of geophysical borehole logs. Comput. Geosci. 60, 34–40.

Gervilla, F., Kojonen, K., 2002. The platinum-group minerals in the upper section of the Keivitsansarvi Ni-Cu-PGE deposit, Northern Finland. Can. Mineral. 40, 377–394.

Geological Survey of Finland – website – resource estimation – http://en.gtk.fi/informationservices/commodities/nickel.html.

Hall, M., Hall, B., 2017. Distributed collaborative prediction: Results of the machine learning contest. Lead. Edge, 267–269.

Hanski, E., Huhma, H., Lehtinen, M., Nurmi, P. A., Rämö, T., Ramo, O. T., and A. Nurmi, P., 2005. Precambrian Geology of Finland, Chapter 4: Central Lapland greenstone belt. 139–193 p.

Hanski, E., Huhma, H., Rastas, P., Kamenetsky, V.S., 2001. The paleoproterozoic komatiite-picrite associations of finnish lapland. J. Petrol. 42, 855–876.

Heggie, G.J., Barnes, S.J., Fiorentini, M., 2013. Application of lithogeochemistry in the assessment of nickel-sulphide potential in komatiite belts from northern Finland and Norway. Bull. Geol. Soc. Finland 85, 107–126.

Hill, E., Robertson, J., Uvarova, Y., 2015. Multiscale hierarchical domaining and compression of drill hole data. Comput. Geosci. 79, 47–57.

Huhma, H., Mänttäri, I., Peltonen, P., Kontinen, A., Halkoaho, T., Hanski, E., Hokkanen, T., Hölttä, P., Juopperi, H., Konnunaho, J., Lahaye, Y., Luukkonen, E., Pietikäinen, K., Pulkkinen, A., Sorjonen-Ward, P., and Vaasjoki, M., 2013. The age of the Archaean greenstone belts in Finland: Tutkimusraportti – Geologian Tutkimuskeskus, pp. 49–51.

Kerr, A., 2001. The calculation and use of sulfide metal contents in the study of magmatic ore deposits; a methodological analysis. Explor. Min. Geol. 10, 289–301.

Le Vaillant, M., Barnes, S.J., Fiorentini, M.L., Santaguida, F., Törmänen, T., 2016. Effects of hydrous alteration on the distribution of base metals and platinum group elements within the Kevitsa magmatic nickel sulphide deposit. Ore Geol. Rev. 72 Part 1, 128–148.

Lightfoot, P.C., Keays, R.R., Evans-Lamswood, D., Wheeler, R., 2012. S saturation history of Nain plutonic suite mafic intrusions; origin of the Voisey's Bay Ni-Cu-Co sulfide deposit, Labrador, Canada. Miner. Deposita 47, 23–50.

Lindsay, M.D., Aillères, L., Jessel, M.W., de Kemp, E.A., Bettes, P.G., 2012. Locating and quantifying geological uncertainty in three-dimensional models: analysis of the Gippsland Basin, southeastern Australia. Tectonophysics. http://dx.doi.org/10.1016/j.tecto.2012.04.007.

Mallat, S., 1991. Zero-crossings of a wavelet transform. IEEE Trans. Inf. Theory 37, 1019–1033.

Mallat, S., Hwang, W.L., 1992. Singularity detection and processing with wavelets. IEEE Trans. Inf. Theory 38, 617–643.

Mallat, S., Zhong, S., 1992. Characterization of signals from multiscale edges. IEEE Trans. Pattern Anal. Mach. Intell. 14, 710–732.

Mungall, J.E., 2002. Kinetic controls on the partitioning of trace elements between silicate and sulfide liquids. J. Petrol. 43, 749–768.

Mutanen, T., 1997. Geology and ore petrology of the Akanvaara and Koitelainen mafic layered intrusions and the Keivitsa-Satovaara layered complex, northern Finland., 395, Geological Survey of Finland.

Mutanen, T., Huhma, H., 2001. U-Pb geochronology of the Koitelainen, Akanvaara and Keivitsa layered intrusions and related rocks. In: Vaasjoki, M., ed., Radiomatric Age Determinations from Finnish Lapland and Their Bearing on the Timing of Precambrian Volcano-Sedimentary Sequences., Spec. Pap. 33, Geological Survey of Finland, pp. 229–246.

Panda, M., Mosher, C., Chopra, A., 2000. Application of wavelet transforms to reservoir-data analysis and scaling. SPE J. 5, 92–101.

Perez-Muñoz, T., Velasco-Hernandez, J., Hernandez-Martinez, E., 2013. Wavelet transform analysis for lithological characteristics identification in siliciclastic oil fields. J. Appl. Geophys. 98, 298–308.

Saalmann, K., Laine, E.L., 2014. Structure of the Outokumpu ore district and ophiolite-hosted Cu-Co-Zn-Ni-Ag-Au sulfide deposits revealed from 3D modeling and 2D high-resolution seismic reflection data. Ore Geol. Rev. 62, 156–180.

Santaguida, F., Luolavirta, K., Lappalainen, M., Ylinen, J., Voipio, T., Jones, S., 2015. Chapter 3.6 - The Kevitsa Ni-Cu-PGE Deposit in the Central Lapland Greenstone Belt in Finland. In: O'Brien, W.D.M.L. (Ed.), Mineral Deposits of Finland. Elsevier, pp. 195–210.

Torrence, C., Compo, G.P., 1998. A practical guide to wavelet analysis. Bull. Am. Meteorol. Soc. 79, 61–78.

Witkin, A., 1984. Scale-space filtering: A new approach to multi-scale description: Acoustics, Speech, and Signal Processing. IEEE International Conference on ICASSP'84, 1984, pp. 150–153.

Yang, S.-H., Maier, W., Hanski, E., Lappalainen, M., Santaguida, F., Määttä, S., 2013. Origin of ultra-nickeliferous olivine in the Kevitsa Ni–Cu–PGE-mineralized intrusion, northern Finland. Contrib. Miner. Petrol. 166, 81–95.